

Ab initio study of the hydrogen abstraction reaction

$$\text{H}_2\text{O}_2 + \text{OH} \rightarrow \text{HO}_2 + \text{H}_2\text{O}$$

M. Bahri^{a,*}, Y. Tarchouna^a, N. Jaïdane^a, Z. Ben Lakhdar^a, J.P. Flament^b

^aLaboratoire de Spectroscopie Atomique Moléculaire et Applications, Département de Physique, Faculté des Sciences, Université Tunis-El Manar, le Belvédère, 1060 Tunis, Tunisia

^bLaboratoire de Physique des Atomes, Lasers et Molécules, CERLA, Université des Sciences et Technologies de Lille 1, 59655 villeneuve-d'Ascq cedex, France

Received 21 July 2003; accepted 18 September 2003

Abstract

Elementary hydrogen abstraction reaction between OH radical and H₂O₂ molecule to yield H₂O and HO₂ molecules has been investigated by ab initio molecular orbital calculations. In addition to the well known reactants and products structures we have located two stationary structures, an intermediate complex OH–H₂O₂ and a transition state H₃O₃ structures. The binding energy of OH–H₂O₂ and the reaction energy are predicted to be, respectively, –3.7 and –31.4 kcal mol^{–1}. The activated complex is found to be more stable than the reactants by 0.9 kcal mol^{–1} and less stable than the intermediate complex by 2.8 kcal mol^{–1}. These results are used to give a tentative explanation of the observed anomalous behavior of the measured rate constant $k(T)$ as a function of temperature T and to try for an interpretation on the physical origin of the two terms in the, non-Arrhenius, fitted expression of $k(T)$ proposed by Hipler et al. $k(T) = [2.0 \times 10^{12} \exp(-215 \text{ K}/T) + 1.7 \times 10^{18} \exp(-14,800 \text{ K}/T)] \text{ cm}^3 \text{ mol}^{-1} \text{ s}^{-1}$ for $240 \leq T \leq 1600 \text{ K}$.

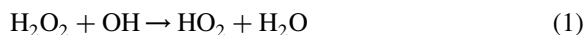
© 2003 Elsevier B.V. All rights reserved.

Keywords: Hydrogen peroxide; Hydroxyl radical; Ab initio

1. Introduction

The hydroxyl radical OH loss and production reactions represent the most important ones in the atmospheric chemistry. OH loss reactions have received considerable attention from experimentalists. One of the important OH reaction is its reaction

with hydrogen peroxide



There have been numerous experimental measurements of the rate constant $k(T)$ of reaction (1) over a wide range of temperature T [1–6]. Ravishankara et al. [1] and Kaufman et al. [2] found that the activation energy E_a of reaction (1), fitted to an Arrhenius expression of $k(T)$, does not exceed 0.5 kcal mol^{–1} and they showed that this negligibly small value of E_a , is qualitatively consistent with exothermicity trends in OH + RH hydrogen abstraction reactions and so they

* Corresponding author. Present address: Département de Physique, Faculté des Sciences, B.P. 802, 3018 Sfax, Tunisia. Fax: +216-4-274437.

E-mail address: mohamed.bahri@fss.rnu.tn (M. Bahri).

suggested that the hydrogen abstraction canal is nearly barrier less and so it is the most probable one for reaction (1). The experimental result of Hipler and Troe [5] shows two remarkable behaviors of $k(T)$: (i) a small temperature dependence for $T < 800$ K and (ii) a strong up-turn at temperature near 800 K. Because this behavior was not previously observed for other OH reactions, the authors call this as ‘anomalous behavior’ of $k(T)$. In a more recent paper [6], the same authors give a two term, non-Arrhenius, fitted expression of the measured rate constant $k(T) = [2.0 \times 10^{12} \exp(-215K/T) + 1.7 \times 10^{18} \exp(-14,800K/T)] \text{ cm}^3 \text{ mol}^{-1} \text{ s}^{-1}$ for $240 \leq T \leq 1600$ K, where the two terms account, respectively, for the two observed behaviors of $k(T)$. To explain this they suggest that a possible intermediate complex participating in reaction (1) is formed. Wang et al. [7] have confirmed the existence of a stable OH–H₂O₂ complex by ab initio and density functional theory (DFT) calculations.

In this work we use ab initio molecular orbital method to study the title reaction considered as an hydrogen abstraction reaction. We search principally for the intermediate complex and transition state structures and for the relative energy of each structure with respect to the reactants. We use our theoretical results to propose an explanation of the observed anomalous behavior of $k(T)$ cited above.

2. Computational method

All ab initio calculations were done with the GAMESS programs [8] using Dunning’s cc-pVTZ basis set [9]. The reactants, products, intermediate complex and the activated complex are taken in their ground state. No symmetry restriction is imposed. The equilibrium geometry, force constant matrix and zero point energy (ZPE) correction for each species are determined at the CASSCF level of calculation. For closed shell systems (H₂O₂, H₂O) we have used an active space including four electrons in four orbitals: the two bonding $\sigma_{\text{O-H}}$ and the two corresponding anti-bonding $\sigma_{\text{O-H}}^*$ orbitals. For open shell systems (OH, HO₂, OH–H₂O₂, H₃O₃) the active space contains, in addition to all $\sigma_{\text{O-H}}$ and $\sigma_{\text{O-H}}^*$ orbitals, the orbital of the unpaired electron of the appropriate oxygen atom. Using the CASSCF

wave function at optimum geometry for each species, the energy was corrected for the remaining electron correlation in a second order perturbation MP2 calculation with the MCQDPT2 method of Nakano [10]. All inactive electrons are included in the MP2 calculations. The basis set superposition error (BSSE) was estimated for both OH–H₂O₂ and H₃O₃ using the Boys–Bernardi counterpoise correction scheme [11]

$$\begin{aligned} \Delta\text{BSSE} &= [E_{\text{X}}^{\text{H}_2\text{O}_2}(\text{H}_2\text{O}_2) + E_{\text{X}}^{\text{OH}}(\text{OH})] - [E_{\text{X}}^{\text{X}}(\text{H}_2\text{O}_2) \\ &\quad + E_{\text{X}}^{\text{X}}(\text{OH})] = [E_{\text{X}}^{\text{H}_2\text{O}_2}(\text{H}_2\text{O}_2) - E_{\text{X}}^{\text{X}}(\text{H}_2\text{O}_2)] \\ &\quad + [E_{\text{X}}^{\text{OH}}(\text{OH}) - E_{\text{X}}^{\text{X}}(\text{OH})] = \Delta\text{BSSE}(\text{H}_2\text{O}_2) \\ &\quad + \Delta\text{BSSE}(\text{OH}) \end{aligned} \quad (2)$$

where X refers to OH–H₂O₂ or H₃O₃, the upper index on the MCQDPT2//CASSCF energy E refers to the basis set and the lower one refers to geometry. $\Delta\text{BSSE}(\text{H}_2\text{O}_2)$ and $\Delta\text{BSSE}(\text{OH})$ are, respectively, the contribution of each fragment H₂O₂ and OH to the ΔBSSE .

3. Results and discussion

3.1. Geometries

The ab initio calculations of the optimized geometry for the reactants (H₂O₂, OH) and the products (H₂O, HO₂) are a simple task, the major difficulty in a such study is the location of the intermediate complex OH–H₂O₂ (Fig. 1a) and the transition state H₃O₃ (Fig. 1b) structures. For this reason we focus in this section on the geometry results of OH–H₂O₂ and H₃O₃.

In Table 1 and Fig. 1 we have reported the geometrical parameters of H₃O₃ and OH–H₂O₂, the later ones are compared to the UMP2 (full)/6-311++G(d,p) ones determined by Wang et al. [7]. According to Fig. 1a we note that the intermediate complex has a five membered ring like structure with two hydrogen bonds. One is the hydrogen bond between (H3, O5) atoms, the other is between (H6, O2) ones. The result of Wang et al. predicts nearly equal lengths for these two H-bonds (2.149 and 2.150 Å) while our calculation shows a slight difference between them (2.355 and 2.398 Å). For the transition state structure result we note that

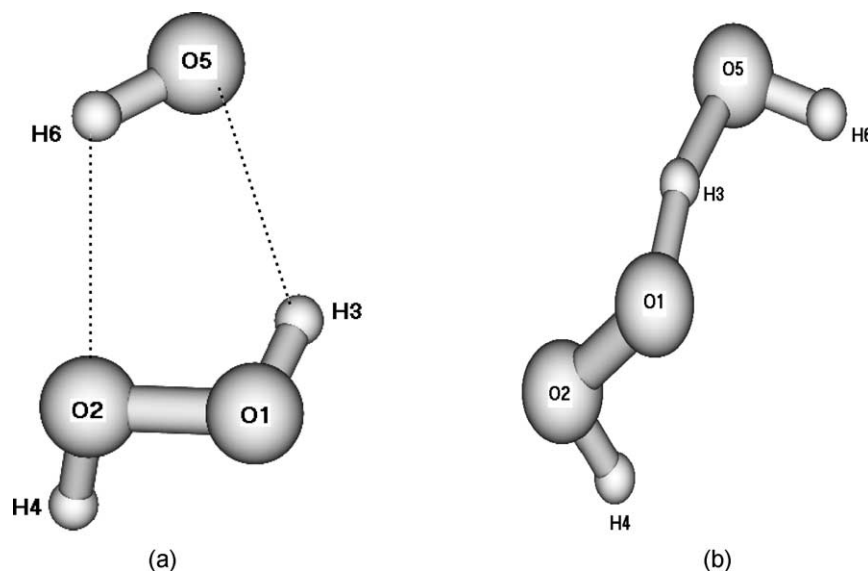


Fig. 1. Geometry of the intermediate $\text{OH-H}_2\text{O}_2$ (a) and the transition state H_3O_3 (b) complexes.

breaking O1-H3 bond is shorter by 0.131 \AA than forming H3-O5 one, while their homologous, respectively, in H_2O_2 and H_2O are nearly equal (0.963 and 0.962 \AA). This means that the transition state has a reactant like character. This is consistent with the exothermic character of reaction (1). A value of 164.3° for the O5H3O1 bending angle indicates that the preferred bringing together of H_2O_2 and OH for hydrogen abstraction reaction is the one where O5 , H3 , O1 atoms are nearly collinear. This has already been observed in other hydrogen abstraction reactions [12–17]. In Fig. 2 we have reported the CASSCF isodensity curves of $\sigma_{\text{O1-H3}}$ in the H_3O_3 activated complex. We note that the probability to find the electrons occupying the $\sigma_{\text{O1-H3}}$ in the region between H3 and O5 atoms is important. So the O1-H3 and H3-O5 bonds at the transition state are ready to be, respectively, broken and formed. This is consistent with the hydrogen abstraction reaction hypothesis and represents the first indication that we have located the adequate transition state structure.

3.2. Frequencies

The calculated CASSCF harmonic frequencies and infrared intensities of the intermediate $\text{OH-H}_2\text{O}_2$ complex are listed in Table 2. Our calculation predicts that there are six strong bands in the infrared

spectrum. They involve three intra-molecular and three inter-molecular vibrational modes. The calculation of Wang et al. [7] predicts also three strong intra-molecular bands but a single inter-molecular

Table 1
Calculated geometrical parameters of the intermediate complex ($\text{OH-H}_2\text{O}_2$) and the transition state H_3O_3

Parameters ^a	$\text{OH-H}_2\text{O}_2$		H_3O_3^b
	This work	Other work ^c	
$R(\text{O1-O2})$	1.386	1.450	(1.385) 1.355 (1.303)
$R(\text{O1-H3})$	0.965	0.969	(0.963) 1.124
$R(\text{O2-H4})$	0.963	0.964	(0.963) 0.965 (0.967)
$R(\text{H3-O5})$	2.355	2.150	
$R(\text{O5-H6})$	0.975	0.973	1.255 (0.962)
$R(\text{O2-H6})$	2.398	2.149	0.974 (0.962)
$\theta(\text{O2O1H3})$	102.8	99.3	(103.0) 104.6
$\theta(\text{O1O2H4})$	103.1	99.9	(103.0) 104.4 (105.8)
$\theta(\text{O5H3O1})$	135.3	139.5	164.3
$\theta(\text{H3O5H6})$	78.5	76.9	98.6 (103.1)
$\alpha(\text{H4O2O1H3})$	107.9	122.6	(107.1) 96.5
$\alpha(\text{O5H3O1O2})$	25.2	11.4	−94.4
$\alpha(\text{H6O5H3O1})$	−5.9	−3.5	−31.9

Bond lengths in \AA , bending θ and torsional α angles in degree.

^a See Fig. 1.

^b Values in parenthesis at the left and /or at the right are respectively the correspondent parameters of reactant and product optimal structures.

^c Ref. [7].

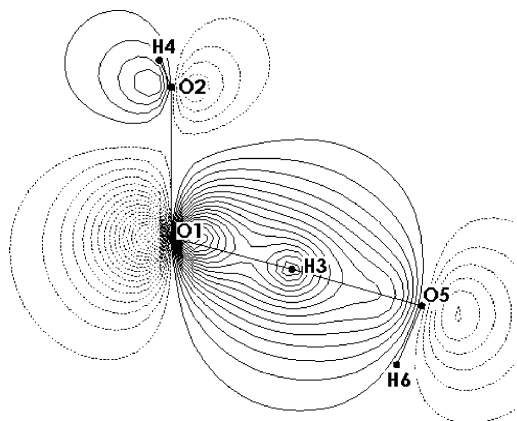


Fig. 2. CASSCF isodensity curves corresponding to the $\sigma(\text{O1}-\text{H3})$ orbital in H_3O_3 .

one. By comparing the frequency values of modes 1–6 for OH and H_2O_2 moieties in OH– H_2O_2 with the corresponding ones in the isolated OH and H_2O_2 molecules, we note that the relative change does not exceed 1%. In spite of the fact that H4 atom is not implied in the hydrogen bonds of OH– H_2O_2 , the frequency and the IR intensity of $\gamma(\text{H4}-\text{O2})$ mode exhibits a significant increase. This can be due to the fact that in OH– H_2O_2 this mode is coupled with $\gamma(\text{H6}-\text{O2})$, which involves the H6 hydrogen atom implied in an hydrogen bond with the H4 atom partner (O2). Such a change of the $\gamma(\text{H4}-\text{O2})$ in the IR spectrum of the pure gaseous H_2O_2 and of

Table 2
Calculated harmonic vibrational frequencies (cm^{-1}) and infrared intensities ($\text{Debye}^2 \text{AMU}^{-1} \text{\AA}^{-2}$) of the intermediate OH– H_2O_2

	Modes	Frequencies	IR intensities
1	$\nu(\text{O2}-\text{H4})$	3751.9 (3765.2) ^a	0.478 (0.480)
2	$\nu(\text{O1}-\text{H3})$	3737.0 (3762.1)	1.444 (0.324)
3	$\nu(\text{O5}-\text{H6})$	3662.3 (3655.0)	0.324 (0.050)
4	$\delta_s(\text{OH})$	1583.3 (1566.7)	0.291 (0.010)
5	$\delta_{as}(\text{OH})$	1486.2 (1478.1)	2.185 (2.210)
6	$\nu(\text{O}-\text{O})$	1158.7 (1159.7)	0.034 (0.020)
7	$\gamma(\text{H4}) + \gamma(\text{H6})$	509.4 (432.6)	5.054 (3.790)
8	Inter-molecular	380.4	2.765
9	Inter-molecular	245.1	1.425
10	Inter-molecular	200.6	4.222
11	Inter-molecular	138.1	0.069
12	Inter-molecular	122.1	0.059

^a Values in parenthesis are those of the isolated H_2O_2 and OH molecules.

Table 3

Contribution (dimensionless) of each internal coordinate in the imaginary normal mode of H_3O_3

Internal coordinate	Contribution
$R(\text{O1}-\text{O2})$	−0.039
$R(\text{O1}-\text{H3})$	0.992
$R(\text{O2}-\text{H4})$	0.014
$R(\text{H3}-\text{O5})$	−1.000
$R(\text{O5}-\text{H6})$	−0.016
$\theta(\text{O2O1H3})$	0.023
$\theta(\text{O1O2H4})$	0.007
$\theta(\text{O5H3O1})$	0.039
$\theta(\text{H3O5H6})$	0.035
$\alpha(\text{H4O2O1H3})$	−0.080
$\alpha(\text{O5H3O1O2})$	0.178
$\alpha(\text{H6O5H3O1})$	−0.164

a (OH, H_2O_2) gaseous mixture, could be a possible experimental proof of the existence of a stable OH– H_2O_2 complex. A second experimental proof which is technically more difficult to be realized, can be the detection of the inter-molecular mode (mode 10 in Table 2) for which our calculation predicts a strong band in the far infrared region (200.6 cm^{-1}).

The Hessian matrix of the transition state possesses only one imaginary frequency which has a magnitude of 4207.4 cm^{-1} . The 11 real frequencies are (in cm^{-1}) 3708.7, 3672.5, 1548.5, 1449.6, 1188.1, 1118.1, 785.5, 454.2, 325.0, 184.7 and 141.4. The imaginary normal mode is decomposed into 12 internal coordinates by the method of Boatz and Gordon [18], the result is given in Table 3. The transition state eigenvector associated with the unique imaginary frequency is primarily a motion of the H3 hydrogen atom between O1 and O5. This represents the second indication that we have located the adequate transition structure in accordance with the hydrogen abstraction reaction hypothesis.

3.3. Energetics

The calculated CASSCF and MCQDPT2 total energies of reactants, products, intermediate OH– H_2O_2 and activated H_3O_3 complexes are listed in Table 4. The total energies used to evaluate the BSSE correction for OH– H_2O_2 and H_3O_3 are listed in Table 5. Inspection of this table shows that: (i) the contribution $\Delta\text{BSSE}(\text{OH})$ of the smallest fragment

Table 4
Total energies (a.u.) of H₂O₂, OH, HO₂, H₂O, OH–H₂O₂ and H₃O₃

Species	This work		Other work ^a
	CASSCF	MCQDPT2//CASSCF	
H ₂ O ₂	–150.8834334 (17.4) ^b	–151.3622410	–151.28332
OH	–75.4382135 (5.2)	–75.6419228	–75.61491
HO ₂	–150.2536076 (9.3)	–150.7231216	
H ₂ O	–76.1023372 (13.4)	–76.3312231	
OH–H ₂ O ₂	–226.3275707 (24.3)	–227.0148594	–226.93082
H ₃ O ₃	–226.2894587 (20.8)	–227.0082482	

^a Ref. [7].

^b Value in parenthesis are the ZPE corrections in kcal mol^{–1}.

OH is more important than the one $\Delta\text{BSSE}(\text{H}_2\text{O}_2)$ of H₂O₂; (ii) including dynamical correlation increases the value of ΔBSSE ; and (iii) the value of ΔBSSE for the intermediate complex is small compared to the one for the transition state involving the same fragments (OH and H₂O₂). In Table 6, we have reported the resulting binding energy D_0 of OH–H₂O₂ compared to the CCSD(T)//MP2 one of Wang et al. [7]. Our calculation predicts, for D_0 , a value of 3.7 kcal mol^{–1} which differs from the one predicted by Wang et al. only by 0.4 kcal mol^{–1}. So our result shows a slightly less stable OH–H₂O₂ complex compared to the one found by Wang et al. In Fig. 3 we have reported the CASSCF and MCQDPT2 diagrammatic schemes of the reaction energetics. The CASSCF result shows a transition state complex less stable than the reactants and the activation barrier is predicted to have a large value (17.5 kcal mol^{–1}). Including dynamical correlation via the MCQDPT2 method the transition state, with

no consideration of ZPE and BSSE corrections, becomes more stable than the reactants by 2.6 kcal mol^{–1}. Before making any interpretation on this result we need, firstly, to test the reliability of our MCQDPT2//CASSCF energy calculations and, secondly, to add ZPE and BSSE corrections. The comparison between calculated and experimental reaction energy E_r and bond dissociation energies $E_D(\text{H}-\text{OOH})$ for breaking H–OOH bond and $E_D(\text{H}-\text{OH})$ for forming H–OH one can be the better test. The MCQDPT2//CASSCF values of E_r , $E_D(\text{H}-\text{OOH})$ and $E_D(\text{H}-\text{OH})$ are listed and compared to experimental ones in Table 7. The calculated values are in excellent agreement with the experimental result. This test supports our MCQDPT2//CASSCF energy calculation. Including ZPE and BSSE corrections the transition state remains energetically below the reactants but only by 0.9 kcal mol^{–1}. Our result predicts that the hydrogen abstraction path for reaction (1) is barrier

Table 5
Total energies (a.u.) used to evaluate the BSSE correction (kcal mol^{–1}) for OH–H₂O₂ and H₃O₃ complexes (see Eq. (2))

	X = OH–H ₂ O ₂		X = H ₃ O ₃	
	CASSCF	MCQDPT2	CASSCF	MCQDPT2
$E_X^{\text{OH}}(\text{OH})$	–75.4382123	–75.6419250	–75.4382135	–75.6419222
$E_X^{\text{H}}(\text{OH})$	–75.4389294	–75.6433366	–75.4391492	–75.6458100
$E_X^{\text{H}_2\text{O}_2}(\text{H}_2\text{O}_2)$	–150.8834278	–151.3623160	–150.8667357	–151.3452644
$E_X^{\text{H}_2\text{O}_2}(\text{H}_2\text{O}_2)$	–150.8837852	–151.3630790	–150.8671988	–151.3468774
$\Delta\text{BSSE}(\text{OH})$	0.5	0.9	0.6	2.4
$\Delta\text{BSSE}(\text{H}_2\text{O}_2)$	0.2	0.5	0.3	1.0
ΔBSSE	0.7	1.4	0.9	3.4

Table 6
Binding energy D_0 (kcal mol⁻¹) of the intermediate OH–H₂O₂ complex

	CASSCF	MCQDPT2	CCSD(T)//MP2 ^a
D_e	3.7 (3.1) ^b	6.7 (5.3)	5.9
D_0	1.3	3.7	4.1

^a Ref. [7].

^b Values in parenthesis are the BSSE corrected ones.

less as it is proposed by Ravishankara et al. This means that if OH and H₂O₂ are brought together in the preferred direction, as described in Section 3.1, no barrier is required for reaction. The rate constant k of such reactive processes (with no barrier) could not have a significant temperature dependence. This is exactly what is observed experimentally for temperatures below 800 K. Then our calculation predicts that the observed small temperature dependence of $k(T)$ for $T < 800$ K is primarily due to the barrier less hydrogen abstraction reaction, which brings H₂O₂

and OH molecules together with an appropriate relative orientation as described in the TS structure. We suggest that some other relative orientations lead to the formation of the intermediate complex OH–H₂O₂. It remains to understand the substantial increase of $k(T)$ for $T > 800$ K.

As it is mentioned in Section 3.1, the OH–H₂O₂ possesses two hydrogen bonds (O5–H3) and (O2–H6). The contribution of each hydrogen bond to D_0 can be estimated to be equal to $D_0/2$ if the two hydrogen bonds have the same length as in the result of Wang et al. Our calculation predicts a bond length of (O2–H6) H-bond slightly longer than the (O5–H3) one. This means that the contribution D_{02} of (O2–H6) H-bond to D_0 is less than the one D_{01} of (O5–H3) H-bond. To estimate D_{02} we can write D_0 as

$$D_0 = D_{01} + D_{02} \quad (3)$$

At the equilibrium geometry the most important contribution in the H-bond interaction is the dispersion which can be modeled by an R^{-6} term [22]

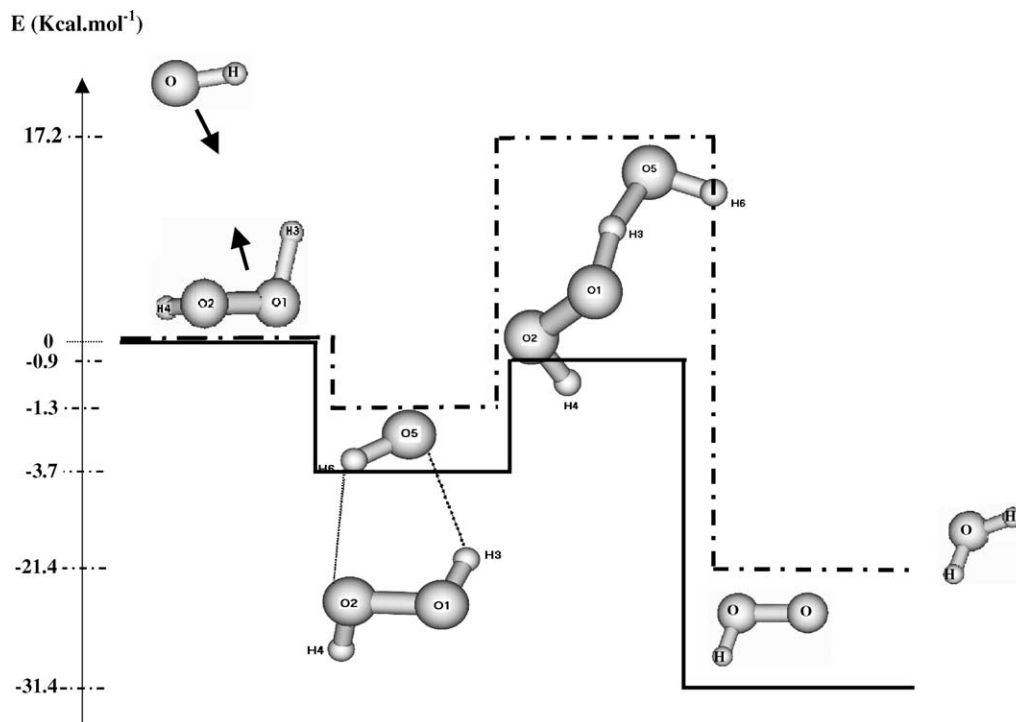


Fig. 3. CASSCF (dotted line) and MCQDPT2 (full line) diagrammatic schemes of the reaction energetics (the indicated values are the BSSE and/or ZPE corrected ones).

Table 7
Reaction and bond dissociation energies (kcal mol⁻¹)

	CASSCF	MCQDPT2// CASSCF	Exp.
E_R	-21.5	-31.5	-31.6 ^a
$E_D(\text{H}-\text{OOH})$	-81.6	-87.4	-87.2 ± 1 ^b
$E_D(\text{H}-\text{OH})$	-103.1	-118.9	-117.59 ± 0.07 ^c

The energy of hydrogen atom calculated at the ROHF level is -0.4998099 a.u.

^a Ref. [19].

^b Ref. [20].

^c Ref. [21].

and we can write approximately:

$$\frac{D_{01}}{D_{02}} \approx \left[\frac{R_{(\text{O2}-\text{H6})}}{R_{(\text{O1}-\text{H3})}} \right]^6 \quad (4)$$

Substituting Eqs. (4) into (3) we obtain

$$D_{02} \approx \frac{D_0}{1 + \left[\frac{R_{(\text{O2}-\text{H6})}}{R_{(\text{O1}-\text{H3})}} \right]^6} \quad (5)$$

Using the values of $R(\text{O2}-\text{H6})$ and $R(\text{O1}-\text{H3})$ from Table 1, we find an approximate value of 1.75 kcal mol⁻¹ (~880 K) for D_{02} .

As reaction (1), has no barrier, it is sufficient for the OH-H₂O₂ complex (Fig. 1a), to be transformed from the stable to the reactive form that acquires a thermal energy via an increase of temperature, and becomes able to break the (O2-H6) H-bond and consequently changes the relative orientation of OH with respect to H₂O₂. The required thermal energy must be equal to or higher than D_{02} ; such a value of the thermal energy can be attained when the temperature becomes equal to or higher than 880 K. Thus from our result we can predict that for temperatures above 880 K some stable OH-H₂O₂ complex can be liberated from the potential well. Increasing temperature can lead to complete dissociation of OH-H₂O₂ complex into OH and H₂O₂ molecules. Having sufficient energy to pass over possible encountered rotational barriers, liberated or/and dissociated ones can reach the TS structure and so undergo the barrier less hydrogen abstraction reaction. Consequently, this can lead to an important increase in the value of $k(T)$ as it is observed experimentally.

We are able now to give a tentative interpretation of the origin of the two terms in the $k(T)$ expression given by Hipler et al.

The first term, having a small temperature dependence represents the contribution to $k(T)$ of the barrier less reactive processes involving H₂O₂ and OH molecules, bringing them together with an appropriate relative orientation and leading, directly, to the products.

The second term, which is important only for high temperatures, represents the contribution of the reactive processes involving the breaking of (H6-O2) H-bond in the intermediate complex and its complete dissociation (into isolated OH and H₂O₂) accompanied by a possible reorientation of OH with respect to H₂O₂ to reach the hydrogen abstraction path of the first process. Using this reasoning we suggest that for sufficiently high temperatures, for which all intermediate complexes are dissociated, only the direct, barrier less, hydrogen abstraction canal is available and so the rate constant, probably, exhibits again the small temperature dependence behavior observed for low temperatures. This remain to be validated by experimental measurement of $k(T)$ for high enough temperatures.

4. Conclusion

We have used ab initio molecular orbital calculations to study the H₂O₂ + OH reaction considered as an hydrogen abstraction reaction. Our results show the existence of two complex structures; an intermediate OH-H₂O₂ and a transition state H₃O₃. The ZPE and BSSE corrected binding energy of OH-H₂O₂ is predicted to be -3.7 kcal mol⁻¹. The imaginary frequency of H₃O₃ has a magnitude of 4207.4 cm⁻¹ and corresponds to the motion of an hydrogen atom between H₂O₂ and OH. After testing the reliability of our MCQDPT2//CASSCF energy calculation and adding ZPE and BSSE corrections, the activated complex is found to be less energetic than the reactants by 0.9 kcal mol⁻¹ and more energetic than OH-H₂O₂ by 2.8 kcal mol⁻¹. The hydrogen abstraction canal for the title reaction is then predicted to be barrier less. These results allow us to suggest the existence of two reactive processes, which contribute to the value of the measured rate

constant $k(T)$ as it is signaled by Hippler et al. Both process involve the barrier less hydrogen abstraction canal.

The first process, which has small temperature dependence, involves the direct reaction bringing OH and H₂O₂ together with an adequate relative orientation. The second, which appears only for high temperatures, involves the breaking of (H6–O2) H-bond in OH–H₂O₂ for $T \sim 800$ K and probably its complete dissociation at higher temperatures accompanied by the reorientation of OH with respect to H₂O₂ and so leading to the barrier less canal as in the first process.

The two described reactive processes give a tentative interpretation of the physical origin of the two terms in the fitted expression of the measured rate constant proposed by Hippler et al.

References

- [1] G.L. Vaghjiani, A.R. Ravishankara, N. Cohen, J. Phys. Chem. 93 (1989) 7833.
- [2] U.C. Sridharan, B. Reimann, F. Kaufman, J. Chem. Phys. 73 (3) (1980) 1286.
- [3] L.F. Keyser, J. Phys. Chem. 84 (1980) 1659.
- [4] A. Mellouki, S. Teton, G. Laverdet, A. Quilgars, G. Le Bras, J. Chim. Phys. 91 (1994) 437.
- [5] H. Hippler, J. Troe, Chem. Phys. Lett. 192 (1992) 333.
- [6] H. Hippler, H. Neunaber, J. Troe, J. Chem. Phys. 103 (9) (1995) 3510.
- [7] B. Wang, H. Hou, Y. Gu, Chem. Phys. Lett. 309 (1999) 274.
- [8] M.W. Schmidt, K.K. Baldrige, J.A. Boatz, S.T. Elbert, M.S. Gordon, J.H. Jensen, S. Koseki, N. Matsunaga, K.A. Nguyen, S.J. Su, T.L. Windus, M. Dupuis, J. Comput. Chem. 14 (1993) 1347.
- [9] T.H. Dunning Jr., J. Chem. Phys. 90 (1989) 1007.
- [10] H. Nakano, J. Chem. Phys. 99 (1993) 7983.
- [11] S.F. Boys, F. Bernardi, Mol. Phys. 19 (1970) 553.
- [12] Y. Tarchouna, M. Bahri, N. Jaïdane, Z. Ben Lakhdar, J.P. Flament, J. Chem. Phys. 118 (3) (2003) 1189.
- [13] M. Bahri, N. Jaïdane, Z. Ben Lakhdar, J.P. Flament, J. Chim. Phys. 96 (1999) 634.
- [14] T.N. Truong, D.G. Truhlar, J. Chem. Phys. 93 (1990) 1761.
- [15] V.S. Melissas, D.G. Truhlar, J. Phys. Chem. 98 (1993) 875.
- [16] K.D. Dobbs, D.A. Dixon, A. Komornicki, J. Chem. Phys. 98 (1993) 8852.
- [17] J.M. Martell, A.K. Mehta, P.D. Pacey, R.J. Boyd, J. Phys. Chem. 99 (1995) 8861.
- [18] J.A. Boatz, M.S. Gordon, J. Phys. Chem. 93 (1989) 1819.
- [19] D.L. Baulch, C.L. Cobos, R.A. Cox, C. Esser, P. Frank, Th Just, J.A. Kerr, M.J. Pilling, J. Troe, R.W. Walker, J. Warnatz, J. Phys. Chem. Ref. Data 21 (3) (1992) 411.
- [20] D.F. McMillen, D.M. Golden, Annu. Rev. Phys. Chem. 33 (1982) 493.
- [21] B. Ruscic, A.F. Wagner, L.B. Harding, R.L. Asher, D. Feller, D.A. Dixon, K.A. Peterson, Y. Song, X. Qian, C.-Y. Ng, J. Liu, W. Chen, D.W. Schwenke, J. Phys. Chem. A 106 (2002) 2727.
- [22] G.A. Jeffrey, An introduction to hydrogen bonding, in: D.G. Truhlar (Ed.), Oxford University Press, New York, 1997.